# Ectons and their Role in Electrical Discharges in Vacuum and Gases

G. Mesyats

*J. PHYS IV FRANCE* 7 (1997)
Colloque C4, Supplément au Journal de Physique III d'octobre 1997 

# Ectons and their Role in Electrical Discharges in Vacuum and Gases

G.A. Mesyats

*Institute of Electrophysics of the Russian Academy of Sciences, 34 Komsomolskaya St., Ekaterinburg 620049, Russia*

**Abstract.** The present paper deals with the short-term bursts – ectons of electrons appearing due to micro-explosions occuring at the cathode surface owing to the high specific energy and the strong overheating of the metal. Ectons play a fundamental role in vacuum arcs and sparks, in low-pressure discharges, in compressed and high-strength gases, etc. i.e., in cases where a high electric field exists at the cathode surface and a high density field emission current is emitted by the cathode or there exists a possibility to produce a high energy density ion a cathode microvolume.

## 1. INTRODUCTION

"Ectons" [1] is formed of the initial letters of the English wording "explosive center". The discovery of ectons is based on the advances in the study of explosive electron emission [2-4]. The term "explosive electron emission" (EEE) refers to the emission of electron current from the surface of a conductor being a cathode as a result of an explosion of the cathode material in a microscopic volume at its surface. The most common way to initiate EEE is to rapidly heat microregions of the cathode by a high-density electric current. The simplest example is the current of field emission (FE) from cathode microprotrusions, whose density at rather high electric fields may reach $10^9$ A/cm$^2$. For a long time it was thought that EEE is initiated only by FE current. Now it is clear that other processes can also be responsible for the initiation of EEE. The electron emission in an ecton generally lasts $10^{-9}$–$10^{-8}$ s and then ceases by itself since the emission center is cooled through heat conduction, a decrease in current density, and ejection of heated metal. To excite an ecton, it is necessary that the specific energy in a cathode microvolume be higher than the sublimation energy (over $10^4$ J/g) with the total energy being $10^{-8}$ J.

## 2. ELECTRICAL EXPLOSION OF METAL AND ECTONS

### 2.1 Electrical explosion of conductors

While on the subject of ectons, we suppose that the metal in a microvolume is subjected to essentially the same processes as in an electrical explosion of a conductor (EEC) [5]. Of greatest interest for us, from the viewpoint of the EEC physics, is the fast heating of the conductor (at a rate of over $10^{13}$ K/s). This forms the basis for studying the physical properties of metals and their phase transformations as they rapidly go through all – from solid to plasma – states. These studies are important to elucidate the behavior of metals in the neighborhood of the critical point, the properties of nonideal plasmas, and the high-temperature metal–nonmetal phase transition [6].

The EEC process can be subdivided into two stages. The initial stage involves the heating of the metal in the solid state, its melting, and the heating of the liquid metal to the onset of vaporization. At this stage, the change in the density of the metal is not essential. This is followed by the stage of explosion where the conductor resistance increases abruptly ($10^2$ or more times). This is due to the

expansion of the conductor and, hence, due to a decrease in its density. For the initial stage of EEC, the state of the metal can be characterized by only one thermodynamic variable such as temperature or specific energy. The resistivity of the conductor at this stage depends only on temperature or specific energy, i.e., the dependence $\kappa(T)$ or $\kappa(w)$ takes place.

The stage of the explosion, as such, is most complicated to study. At this stage, a number of phenomena develop that add complexity to the physical mechanism of EEC. Among these phenomena are instabilities, shunting discharges, stratification, and the like. A feature of this stage is that the resistance is not a single-valued function of energy density but depends on power density [5].Besides experimentation, there are three other methods of attack for the EEC problems: numerical simulation, simplified calculations using models, and similarity techniques. In EEC calculations using similarity techniques, an important role is played by the specific integral of action (specific action) defined as

$$\bar{h} = \int_0^{t_d} j^2 dt, \tag{2.1}$$

where $j$ is the current density and $t_d$ is the time delay to explosion.

Table 1 presents experimental values of the specific action for various conductors with the initial temperature being room temperature and the highest energy density being $10^8$ A/cm$^2$ ($\bar{h}_1$) and with the initial temperature equal to the melting temperature ($\bar{h}_2$) [7]. The weak dependence of $\bar{h}$ on $t$ and $j$ for $j \leq 10^7$ A/cm$^2$ has also been noted in other works. Some of them are reviewed in [8]. Sometimes, the specific action is roughly estimated in terms of a classical approach assuming that the explosion occurs within one stage as a certain critical temperature, $T_{ex}$, has been achieved. If we assume that the resistivity is given by $\kappa=\kappa_0 T$, and the heat capacity $c$ is temperature independent, we obtain

$$\int_0^{t_d} j^2 dt = \frac{\rho c}{\kappa_0} \ln \frac{T_{ex}}{T_0} = \bar{h}, \tag{2.2}$$

where $T_0$ is the initial temperature and $\rho$ is the density of the conductor material.

Table 1.

| Material | Al | Ag | Au | Cu | Ni | Fe | W |
|---|---|---|---|---|---|---|---|
| $\bar{h}_1$, $10^9$ A$^2$·s/cm$^4$ | 1.8 | 2.8 · | 1.8 | 4.1 | 1.9 | 1.4 | 1.8 |
| $\bar{h}_2$, $10^9$ A$^2$·s/cm$^4$ | 1.4 | 2.0 | 1.3 | 3.0 | 1.6 | 1.2 | 1.4 |

Attention must be given to the fact that the specific action $\bar{h}$ depends on the initial temperature of the conductor $T_0$. Recall that the data in Table 1 have been obtained for the initial temperature being room temperature and for the melting temperature.

### 2.2 The simplest model of an ecton

The simplest ecton model is constructed based on the energy balance equation for a conical point. Therefore, formula (2.2) can be used. The heat conduction in the point is ignored since the process is short-term. It is assumed that the electron emission in the ecton ceases due to the cooling of the emission center. The center is considered cool when the Joule heating radius becomes equal to the heat conduction radius. Eventually, this has the results as follows [10]. The ecton operation time is given by

$$t_e = i^2/(\pi^2 a^2 \bar{h}\, \theta^4). \tag{2.3}$$

where $\theta$ is the cone angle, $a$ is the diffusivity, $i$ is the current. The mass of the metal removed in the process of explosion will be

$$m_e = 2\rho i^3/[3\pi^2 (a\bar{h})^{3/2} \theta^4]. \tag{2.4}$$

The electron charge removed by the ecton will be

$$n_e = i^3 / \pi^2 a^2 \bar{h} e \theta^4, \tag{2.5}$$

where $e$ is the charge of an electron. The mass per unit charge removed from the cathode will be given by

$$\gamma_m = \frac{2}{3}\rho\left(\frac{a}{\bar{h}}\right)^{1/2} \tag{2.6}$$

It follows that in terms of this model, the specific mass removed from a cathode by explosion depends only on the properties of the cathode material. After explosion, the plasma produced starts expanding. We have proposed [4] a model for adiabatic plasma expansion. Let a specific energy $w_0$ be introduced into a certain volume of a cathode. This energy, in the process of plasma expansion, converts to the kinetic energy of the plasma particles. For the plasma radius becoming much larger than the characteristic dimension of the initial volume, from the condition that the total energy is conserved in the particle volume it follows that the velocity of propagation of the leading layers of the plasma, v, is related to the specific energy $w_0$ as

$$v = \left(\frac{4\gamma}{\gamma - 1} w_0\right)^{1/2}, \tag{2.7}$$

where $\gamma$ is the adiabatic exponent. For an expanding plasma we have $\gamma = 1.24$ [11]. The plasma expansion velocity is $(1–2)\cdot10^6$ cm/s for W, Mo, Cu, Al, Ni, Pb, and other metals. Therefore, the specific energy prior to a microexplosion is $w_0 = (2–8)\cdot10^4$ J/g. The same values $w_0$ have been obtained from a numerical simulation of a cathode spot [12]. The plasma produced as a result of a microexplosion contains, depending on the metal type, singly, doubly, and even triply charged ions. These ions have rather high energies. For instance, singly charged ions of copper having a velocity of $1.5\cdot10^6$ cm/s are accelerated to 70 eV. Let us discuss the reason for the current cutoff in an ecton. This problem is closely related to the mechanism for the electron emission from a metal. This emission seems to be thermal electron emission enhanced, through the Schottky effect, by the electric field at the metal–plasma interface. In terms of the classical heat model it can be assumed that the temperature may become much higher than the boiling temperature within a time of the order of $10^{-9}$ s. If we believe that the Richardson–Schottky formula is valid for these conditions, we have

$$j = AT^2 \exp\left(-\frac{e\varphi - \alpha E^{1/2}}{kT}\right), \tag{2.8}$$

where $j$ is the electron current density (A/cm$^2$), $A = 120.4$, $T$ is the temperature of the cathode (K), $\varphi$ is the work function ($\varphi = 4.4$ eV for copper), $\alpha = 3.79\cdot10^{-4}$, $E$ is the electric field at the emitting surface (V/cm), and $k$ is Boltzmann's constant.

A simulation of the processes occuring in an ecton has shown that the electric field $E$ is not over $10^5$ V/cm [5]. According to estimates for copper, for the input energy equivalent to $10^4$ K, the current density will be of the order of $10^8$ A/cm$^2$, while for $7\cdot10^3$ K it will be only $5\cdot10^6$ A/cm$^2$, i.e., as the ecton zone is cooled by 30 %, the current density decreases 20-fold. Thus, the qualitative pattern of the current cutoff in an ecton is as follows: Initially, as the ecton has been initiated, the current density is about $10^9$ A/cm$^2$. The cathode material in a microvolume is heated and then explodes, which gives rise to intense thermal electron emission. As the explosion is developing, there take place an increase in the size of the emission zone, heat removal by conduction, and heat removal through evaporation and ejection of the heated liquid metal. All this reduces the temperature in the ecton operation zone and the current density of the thermal electron emission. The decrease in emission current density results in a more rapid cooling of the emission zone due to the Joule heating becoming less intense.

## 3. ELECTRODE SURFACE CONDITION

In the initiation of an ecton, an important role is played by three types of imperfectness of the cathode surface: microprotrusions, adsorbed gases, and dielectric inclusions and films. The irregularities present on the cathode surface [13, 14] are due to various factors such as mechanical treatment, heating, the electric field present at the surface, electrical discharges, *etc.* (Fig. 1). The irregularities on the surface of a metal are especially large when threadlike crystals appear [15] whose height-to-radius ratio may be over $10^3$. Such crystals are formed on the surfaces of electrodes on condensation of oversaturated vapors. In

vacuum, the cathode microrelief is changed substantially by electrical discharges. The discharge current, through thermal processes, produces erosion of the electrodes, which is accompanied by the formation of craters and microprotrusions. To characterize the cathode surface quantitatively, the notion of electric field enhancement is introduced, and the field enhancement factor is denoted as $\beta_E$. This factor is the ratio of the true value of the electric field at the protrusion tip to its average macroscopic value. For $\beta_E \geq 1$, the relation $\beta_E \approx h/r$ can be used [13].

A way of determining the field enhancement factor is measuring the field emission current in vacuum as a function of the electric field. The FE current from a point is described by the Fowler–Nordheim equation

$$i = A\frac{\beta_E^2 E^2 S_{em}}{\varphi}\exp\left(-B\frac{\varphi^{3/2}}{\beta_E E}\right), \qquad (3.1)$$

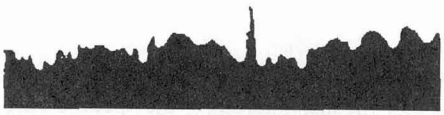

Fig. 1. Cathode surface microrelief [1].

where $A$ and $B$ are the constants entering the Fowler–Nordheim formula, $E$ is the average electric field, $S_{em}$ is the emission area, and $\varphi$ is the work function. As follows from Eq. (3.1), the plot of $\log(i/E^2) = f(1/E)$ should be a straight line. So, for a known work function $\varphi$, we can estimate $\beta_E$ from the slope of the straight line and $S_{em}$ from the portion of the $y$-axis intercepted by the straight line. The field enhancement factor may vary over a wide range (from 10 to $10^2$) [9]. Many researchers, however, believe that the values of the order of $10^3$ are too high; nevertheless, points with these $\beta_E$ values are actually observed on cathode surface. Therefore, additional investigations are needed to explain this contradiction. An important role in the initiation of ectons at a cathode is played by the gas adsorbed on its surface. The phenomenon of surface adsorption is the absorption of a gas or vapors by the surface of a solid. From the chemical viewpoint, an adsorbent has on its surface atoms with an unsaturated valency. This means that the surface of a solid body has some regions where chemical binding with adsorbed particles is provided. Particles in numbers sufficient for all surface bonds to be saturated form a monolayer. This corresponds to the density of adsorbed atoms of the order of $10^{14}$ cm$^{-2}$ [16]. The binding between adsorbed particles in the monolayer is effected by chemical forces. Therefore, this type of adsorption is referred to as chemical adsorption or chemosorption. In chemical adsorption, the binding energy is rather high enough and reaches several electron-volts per particle.

In the environment of a gas capable to oxidize electrodes, the cathode surface turns out to be coated with an oxide film. Moreover, the cathode surface may contain contaminants and dielectric inclusions remained after polishing as well as dielectric inclusions having present in the cathode bulk and exposed on the surface on electrochemical polishing or ion etching [17]. At rather high electric fields induced by the electric charge of ions, breakdown may occur inside the dielectric film. If the resistivity of the dielectric film present on the cathode surface is high, its outer surface is charged by the flow of positive ions onto the cathode. As the breakdown electric field is achieved, the film is broken down and the cathode is damaged at the site of breakdown. Some models [18, 19] use as a criterion for breakdown the achievement of a certain critical FE current density at which a microprotrusion and the adjacent regions of the dielectric are heated and explode. The process under consideration is an act of excitation of an ecton at the surface of a metal.

## 4. THE ROLE OF ECTONS IN VACUUM BREAKDOWN

### 4.1 General considerations

Ectons play an important role in electrical discharges in vacuum. A vacuum discharge involves a vacuum breakdown, a vacuum spark, and a vacuum arc. Vacuum breakdown, i.e., failure of a vacuum insulation, ecton. A vacuum spark and a vacuum arc represent the behavior of ectons in non-steady-state conditions, such that the current in the gap is growing, and in steady-state conditions, reflects the mechanism for the

initiation of an respectively.

Figure 2 presents electro-optical photographs of the evolution of a glow in a gap in the process of a vacuum discharge [4]. They were taken for a pulse generator charged to a voltage $V_0$ which was discharged through a resistor of resistance $R$. Three phases of the process can be distinguished: (1) There is no glow in the gap. This is the stage of breakdown during which energy concentration in a cathode microvolume takes place (Photo I). (2) A glow appears in the gap initially at the cathode and then at the anode. This is the spark stage (Photos from IIth to IXth). The cathode glow testifies to the appearance of an ecton, the ending of the breakdown phase, and the beginning of the spark stage. The number of microexplosions varies from photo to photo. The microexplosions have a random character. The cathode plasma propagates toward the anode with a velocity of ~$2 \cdot 10^6$ cm/s. In Photo VI, the appearance of a glow at the anode is seen. This is the result of the heating of the anode by the current of explosive electron emission. (3) When the cathode and the anode plasmas close the gap, the discharge goes to the arc phase (Photo X). In the spark phase, the current grows to its peak value $i_a = V_0/R$.

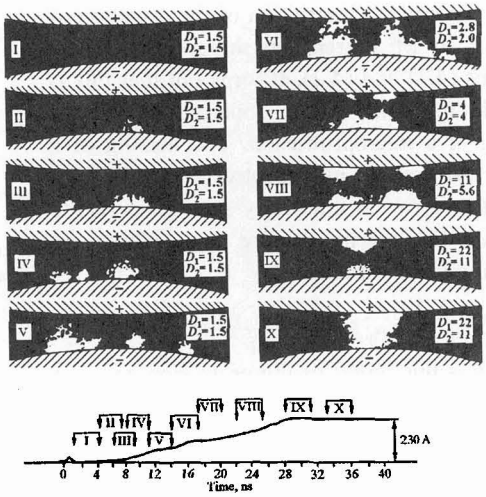


Fig. 2. Typical photographs of the glow in a copper electrode gap, corresponding to different stages of breakdown development ($d$ = 0.35 mm, $V_0$ = 35 kV, $D_1$ and $D_2$: lens apertures). The pictures are taken of different discharges.

So, we will believe that the processes occurring in breakdown lead to concentration of energy in a cathode microvolume, and this energy reaches values sufficient for the material in the microvolume to explode and for an ecton to appear. By a spark we will mean the process from the beginning of a microexplosion at the cathode to the instant the current reaches its highest value determined by the applied voltage and the circuit resistance. The following steady-state operation of the discharge will be referred to as an arc. With that, we suppose that the spark and the arc currents are high enough for the process to be self-sustaining.

### 4.2 The vacuum breakdown

The processes occurring in a vacuum breakdown strongly depend on the surface condition of the electrodes and on the quality of the vacuum. With thoroughly cleaned electrode surfaces and a high-grade vacuum, breakdown occurs due to the current of the field emission proceeding from cathode microprotrusions, and to the Joule heating and further explosion of the microprotrusions. The evidence for this is as follows: The numerous experimental data reviewed in [4] show that for the above conditions, there are two criteria for the appearance of a spark: For the mode where a dc voltage is applied to the gap we have [4]

$$j = \text{const}_1 \tag{4.1}$$

and for the pulsed mode [3, 4]

$$\int_0^{t_d} j^2 dt = \text{const}_2, \tag{4.2}$$

where $j$ is the FE current density at the tip of a microprotrusion, $t_d$ is the time delay to explosion, and the constants characterize the cathode material and the shape of the microprotrusion. Relation (4.1) implies that the electric field at the surface of microprotrusions remains unchanged irrespectively of the gap spacing. This follows from the data reported in [20-22] and summarized in Fig. 3.

A theoretical description of the initiation of an ecton by FE current has the goal to explain relations (4.1) and (4.2). It turns out that this is possible in terms of the Joule model of the heating of a microprotrusion. The heating of a cylindrical cathode microprotrusion by the FE current it carries in the steady state gives rise to a threshold current density and subsequent explosion provided that

$$j = \frac{1}{h}\sqrt{\frac{\lambda}{\kappa_0}}, \qquad (4.3)$$

where $h$ is the height of the protrusion and $\lambda$ is the heat conductivity. Thus, for a protrusion of height 1 μm, the current density $j$ is $2\cdot10^8$, $0.5\cdot10^8$, and $0.25\cdot10^8$ A/cm$^2$ for copper, tungsten, and nickel, respectively. With short pulses, the threshold FE current density is higher than that for the steady-state case. If the pulse duration $t_p$ is much shorter than the time required for a discharge to go to the steady state, the relation

$$t_p << \frac{h^2 \rho c}{\lambda} \qquad (4.4)$$

is valid. For instance, if for tungsten we have $h$ = 0.6 μm, relation (4.4) is satisfied even with $t_p$ = 10 ns. For condition (4.4) fulfilled, the temperature of a cylindrical emitter increases with time by an exponential law:

$$T = T_0 \exp\frac{\kappa_0 \int_0^{t_d} j^2\, dt}{\rho c}. \qquad (4.5)$$

Let the current density be invariable in time. If we assume by convention that a protrusion will explode as a certain critical temperature, $T_{ex}$, is reached, the time delay to explosion will be determined from relation (2.2), which is similar to relation (4.2). Thus, the simple Joule model for the heating of protrusions offers an adequate explanation of the principal experimental criteria given by Eqs. (4.1) and (4.2). It should be noted that these are criteria for the appearance of a spark rather than criteria for breakdown. These criteria yield the time $t_d$ being the duration of the breakdown stage.

To pass from relations (4.1) and (4.2) to the dependence between the time $t_d$ and the electric field $E$, we write an approximation of the Fowler–Nordheim formula:

$$j = A\frac{E^2}{\varphi}\exp\left(-B\frac{\varphi^{3/2}}{E}\right), \qquad (4.6)$$

Here, $j$ is the current density (A/cm$^2$), $A = 1.55\cdot10^{-6}$ (A), $E$ is the electric field (V/cm), $B = 6.85\cdot10^7$, and $\varphi$ is the work function of an electron outgoing from the metal. Formally, formula (4.6) suggests that the electron current density may reach $10^{10}$ A/cm$^2$ and even more. However, even when the current density is as low as of the order of $10^8$ A/cm$^2$, the dependence $j(E)$ shows a departure from the F–N theory which is reflected in a less intense rise of the emission current (Fig. 4) [23]. It turned out that this effect is inherent in all investigated metals such as W, Mo, Ta, Re, *etc.* The above departure is the greater, the higher is the current density and the lower the work function. This effect is due to the influence of the space charge of the emitted electrons. With high electric fields and current densities, the influence of the space charge on the character of the dependence $j(E)$ is predominant. In this case, the dependence $j(E)$ is governed by the

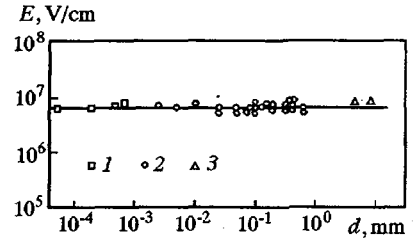


Fig. 3. Local breakdown field at cathode versus electrode separation for tungsten electrodes. Data from [20] (*1*), [22] (*2*), and [21] (*3*).

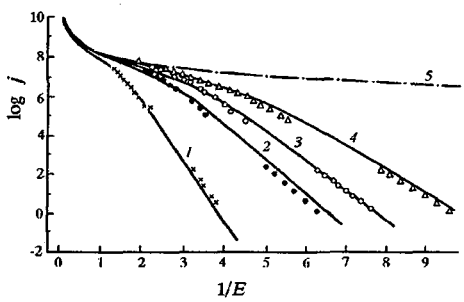


Fig. 4. Comparison of experimental data with predictions of an FE theory, taking account of space charge. Work function $\varphi$ = 4.50 (*1*), 3.19 (*2*), 2.80 (*3*), and 2.44 eV (*4*); (*5*) the Child–Langmuir curve [23].

Child–Langmuir law which is written as [24]

$$j = \frac{4}{9}\varepsilon_0\left(\frac{2e}{m}\right)^{1/2} E^{3/2} r_{em}^{-1/2}, \tag{4.7}$$

where $\varepsilon_0$ is the dielectric constant, $e$ and $m$ are the electron charge and mass, respectively, and $r_{em}$ is the radius of the emitting surface. Dependence (4.7) is presented in Fig. 4 by curve *5*. Investigations of many researchers have demonstrated that with voltage pulses of duration $10^{-9}$–$10^{-6}$ s applied to a tungsten emitter, one can achieve current densities of up to $10^9$ A/cm$^2$ [4,25]. High current densities cause microemitters to explode. If $j$ remains unchanged within the time $t_d$ and the current density is determined by the F–N formula, we have

$$t_d = \frac{\bar{h}}{A^2 E^4 \varphi^2} \exp\left(\frac{2B\varphi^{3/2}}{E}\right), \tag{4.8}$$

where $A$ and $B$ are constants depending on the work function of the material and $E$ is the electric field at the tip of the protrusion. Equation (4.8) demonstrates a strong dependence of $t_d$ on $E$. This strong dependence takes place only at comparatively low fields at the protrusion surface when $j \le 10^8$ A/cm$^2$.

At high values of the current density, the latter is limited by the electron space charge in the region adjacent to the protrusion. Therefore, we have $t_d \propto E^3$, which is confirmed experimentally (Fig. 5) [4]. Thus, measurements of $t_d$ have confirmed that the delay to the appearance of EEE current is due to the delay of the onset of a microexplosion at the cathode and that the value of $t_d$ depends only on the field $E$, which is confirmed experimentally [4]. For a liquid-metal cathode, its surface structure is destroyed under the action of electro-static forces. Tonks [26] considered the balance of the surface tension, gravity, and electrostatic forces. The condition that a horizontal liquid-metal surface is unstable has the form

$$\varepsilon_0 \frac{E^2}{2} > \frac{\alpha}{r} + \rho g r, \tag{4.9}$$

where $\rho$ is the density of the material, $\alpha$ is the coefficient of surface tension, $g$ is the gravitational acceleration, and $r$ is the radius of the liquid surface. The lowest value of $E$ at which the liquid surface is destroyed corresponds to an optimal value of $r = r_0$, such that inequality (4.9) becomes an equality. Thus, for mercury the electric field at which the surface starts destroying is 53 kV/cm and $r_0$ is 0.37 cm [27]. When inequality (4.9) is fulfilled, a hump startsgrowing on the liquid-metal surface. The electric field at its surface increases, which leads to a larger extension of the liquid at this place. Initially, the hump has a nearly spherical segment shape (Fig. 6) and then it transforms to a cone. With that, the tip radius decreases. A protrusion like this can explode under the action of FE current. Thus, for the case of a liquid-metal cathode, the breakdown process involves extraction of a microprotrusion from the liquid metal. To summarize, under ideal conditions where only microprotrusions are present on the cathode surface and there are no contaminants and adsorbed gas, the appearance of the first ecton results from the energy concentration in a cathode microvolume due to the Joule heating of the cathode microprotrusions. In this case, the principal processes in the breakdown are the passage of FE current and the heating of microprotrusions prior to explosion.

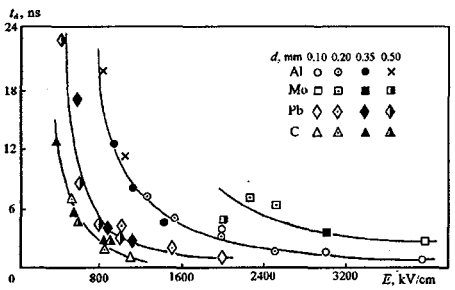


Fig. 5. Time delay to breakdown versus average electric field for electrodes made of various materials.

However, there is a great deal of experimental data which suggest that other breakdown mechanisms also exist [4, 28]. Let us take a brief look at them.

1. The FE electrons are accelerated in the vacuum gap and transfer their energy to a region of the anode surface causing its heating and vaporization and gas desorption from the anode. This leads to the appearance of a flow of plasma and ions from the anode to the cathode.

2. The metal and impurity particles weakly attached to the electrodes, under the action of the voltage applied to the gap, when hitting the opposite electrode, may create conditions for breakdown (heating and evaporation of the particles, deformation of the electrode surface, gas desorption, *etc.*
3. Under the action of the ponderomotive forces of the electric field, changes of the electrode surfaces may occur, namely, formation of micropoints, breakoff of material pieces, deformation of the surface of liquid metals, *etc.* Thereafter, the first or the second mechanism comes into effect.
4. The nonmetal inclusions and films present on the cathode may become efficient emission centers because of the decrease in the work function of the cathode metal or of the breakdown of inclusions and films which plays the role of a trigger discharge.
5. Gas desorption from the electrode surfaces favors the appearance of a gas discharge initiating the breakdown of the vacuum gap.

In our opinion, all these mechanisms, forced initiation included, eventually lead to energy concentration in a cathode microvolume, explosion of the material in this microvolume, and formation of an ecton. Two criteria are necessary for the ecton process to be self-sustaining: the required energy density, $w_0$, and critical mass, $m_0$, formed as a result of the explosion. For some metals ( Cu, Al, Ag ) the criteria are approximately follows:

$$w_0 \approx 5 \cdot 10^4 \text{ J/g}; \qquad m_0 \approx 10^{-13} \text{ g} \tag{4.10}$$

A fundamental role in the process of energy concentration is played by the plasma generated at the cathode. Let us consider this process in more detail.

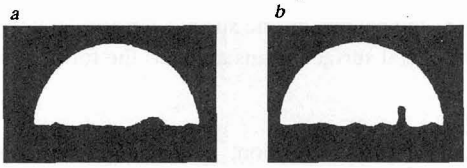


Fig. 6. Microprotrusions on a mercury surface grown at different electric fields between electrodes. The field in case (*a*) was lower than in case (*b*).

### 4.3 Plasma initiation of breakdown

It is well known that a vacuum discharge can be initiated by supplying plasma to the cathode. This process strongly depends on the dielectric films and inclusion present on the cathode. The formation of ectons under the action of the plasma produced by a plasma gun is described in [4]. The plasma arrived at the nearly placed cathode. Ectons appeared when dielectric contaminants were obviously present on the cathode surface. This testifies to the energy concentration in a cathode microvolume. The most probable appearance of an ecton was at a distance less than 100 μm. The probability was the higher, the closer the plasma source was located. With that, the lowest plasma density was $10^{16}$ cm$^{-3}$. For thoroughly cleaned and degassed cathodes, the appearance of ectons was not observed. Ectons were observed to appear at a very short distance from the plasma source to the cathode (about 5 μm), when the cathode surface had been thoroughly cleaned from oxides and dielectric impurities [29]. In this zone, the plasma density was of the order of $10^{20}$ cm$^{-3}$ and the ion current density at the cathode was of the order of $10^7$ A/cm$^2$. The formation of new ectons at a short distance (of the order of several micrometers) was judged from the current waveform and by the appearance of microcraters. What are the reasons for these effects? When plasma is flowing over the surface of a cathode in the presence of an electric field, there takes place the effect of enhancement of the current density at the cathode microprotrusions.

Let us consider three configurations of a microprotrusion on a plane cathode: a cylinder, a cone, and a sphere (Fig. 7). If such a microprotrusion is flown up with plasma, an ion current $i_i = j_i S$ (with $j_i$ being the ion current density and $S$ the surface area of the protrusion) will flow over the protrusion surface. When the current will enter the cathode, the area through which it will pass equals $\pi r^2$ for all three microprotrusion geometries. So the current density at the cathode will be

$$j = j_i S / \pi r^2. \tag{4.11}$$

The area $S$ will be $2\pi rh$, $\pi rl$, and $4\pi R^2$ for a cylinder, a cone, and a sphere, respectively (with $l$ being the generatrix of the cone). With that, the current density enhancement factor, $\beta_j$, will be, respectively, $2h/r$,

$l/r$, and $4R^2/r^2$.

The effect of current density enhancement holds not only for an ion current but also for any current emitted or received by the cathode surface. For instance, if the cathode surface is heated to a high temperature, the surface of a cathode microprotrusion will emit a thermal field emission current whose density in the cathode region will be $\beta_j$ times higher than the density averaged over the surface area. This conclusion is also valid for the backward current of the plasma electrons flying toward the cathode. The above effect is important for the self-sustaining of microexplosive processes, i.e., for the appearance of secondary ectons. Moreover, if irregularities are in the close vicinity of an explosive center, the ion current density at them may be rather high, which, in view of the effect of its enhancement, leads to a microexplosion at the cathode surface. Actually, the ion current density is given by

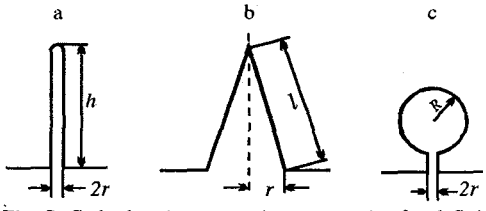


Fig. 7. Cathode microprotrusion geometries for definition of the coefficient of current density enhancement: cylinder (*a*), cone (*b*), and sphere (*c*).

$$j_i = q_i n_i v_i/4, \tag{4.12}$$

where $q_i$ is an average charge of the ions, $n_i$ is their density, and $v_i$ their velocity. Since the ion density decreases with distance $x$ from the emission center as $n_i \propto 1/x^2$, one should expect that the effect of current density enhancement will be strong near the emission center [29].

The influence of the cathode plasma on the energy concentration in a cathode microvolume becomes much more pronounced when a dielectric film or a dielectric inclusion is present on the cathode surface. Let a dielectric film be present on the surface of a cathode with a metal microprotrusion located beneath the film. If this system is in an electric field and plasma arrives at the dielectric surface, the ions moving toward the dielectric film will charge it. The electric field in the film will be

$$E = j_i t/\varepsilon\varepsilon_0, \tag{4.13}$$

where $\varepsilon$ is the permittivity of the film and $t$ is the time. As the electric field reaches a certain value, the film is broken down. The breakdown current will give rise to an ecton. Thus, we have shown that there are two ways of the plasma-assisted initiation of ectons. One of them is associated with the charging of dielectric films and inclusions on the cathode by the plasma ions and the other with the enhancement of the current density at cathode microprotrusions.

If we assume that an ecton is formed with the electric field inside the dielectric $E > 10^6$ V/cm, then, in order that the dielectric film be charged and broken down within a time $t < 10^{-9}$ s, the relation

$$n_i v_i > 10^{23}\ \text{cm}^{-2}\text{s}^{-1} \tag{4.14}$$

must be satisfied. For $v_i \sim 10^6$ cm/s and $n_i \sim 10^{17}$ cm$^{-3}$, the appearance of ectons under the plasma arrived at the cathode can be expected. For the second way of the plasma-assisted initiation of ectons, with the current density being $10^9$ A/cm$^2$, the relation

$$n_i v_i > 10^{28}\ \beta_j^{-1}, \tag{4.15}$$

should be fulfilled. If we suppose that $\beta_j \approx 10^2$–$10^3$, then, in order that ectons be initiated, it is necessary that, provided that the ion density be the same, the plasma density should be two or three orders of magnitude higher [1]. This explains why an ecton can readily be initiated with a low-density plasma at a contaminated cathode, while at a cleaned cathode an ecton is initiated only with a high plasma density (of the order of $10^{20}$ cm$^{-3}$). Other methods for the initiation of breakdown are eventually reduced to the creation of plasma at the cathode. For instance, a general way is to focus laser radiation onto the cathode surface [13, 30, 31]. The appearance of plasma is observed when the radiation energy flux density is in the range 0.01–10 J/cm$^2$. This energy is insufficient for the cathode metal to explode but sufficient for a plasma blob to appear at the cathode. This action causes a heating of the cathode surface, gas desorption, evaporation of the metal, and thermal electron emission. This leads to ionization of the vapor by hot

electrons. For instance, thermal electron emission from the surface of tungsten was observed when the intensity of irradiation was over $2.5 \cdot 10^7$ W/cm$^2$ with the laser pulse duration 50 ns. The thermal electron current density was 0.5 A/cm$^2$. The cathode plasma generated by laser radiation gives rise to an ecton and leads to vacuum breakdown. The adsorbed gas present on the cathode encourages the process of breakdown. The influence of the adsorbed gas on the initiation of ectons is twofold: On the one hand, this gas affects the work function of the metal and thus participates in the initiation of ectons by FE current and, on the other hand, after desorption and ionization, it acts on the metal like plasma. With electric fields $E \geq 10^7$ V/cm, field desorption takes place.

In our view, ectons also appear when a microscopic material particle accelerated to a high velocity hits a cathode. With that, three options for the initiation of an ecton can be qualitatively distinguished. If the velocity of the particle is not very high, its impact on the cathode results in a heating of a cathode microregion, gas desorption and evaporation of the cathode material in this microregion and of the particle itself, ionization of the gas and the vapor, and appearance of an ecton due to the plasma–cathode interaction. At a high velocity, the particle may give rise to a microexplosion and to produce an ecton on its direct interaction with the cathode.

## 5. THE VACUUM SPARK

The vacuum spark most clearly shows up the properties of ectons and EEE under non-steady-state conditions. The role of EEE in a vacuum spark was identified based on the results of a three series of experiments performed using nanosecond high-voltage pulses [4]. First, the electron current at the initial stage of a vacuum spark was investigated. Second, the cathode and anode glows were observed using an electron-optical image converter with nanosecond exposure times and light amplification up to $10^6$ times. Third, the character of the cathode and anode erosion was investigated and the mass of the material removed from their surfaces was measured. Let us discuss in detail the results obtained.

All experiments were performed with a nanosecond pulse generator. The current rise proceeds within a time interval which involves the time delay, $t_d$, and the closure time, $t_c$ [4] (Fig. 8). The time $t_c$ is generally taken as the time between the points where the current makes up 0.1 and 0.9 of its amplitude value, $i_a$, defined as $V_0/R$, where $V_0$ is the voltage amplitude and $R$ is the resistance of the discharge circuit. The time $t_d$ is associated with the breakdown phase, $t_c$ with the spark phase, and the subsequent time with an arc discharge. The electrodes used in the experiments were made of copper, aluminum, tungsten, molybdenum, steel, lead, and graphite; the gap spacing, $d$, was varied from 0.1 to 1 mm.

The conclusions made about the time $t_c$ for plane electrodes are as follows: The closure time $t_c$ increases linearly with gap spacing and does not depend on the amplitude of the applied voltage. The current rise rate $di/dt$ decreases with increasing gap spacing and increases with voltage. The ratio $d/t_c$ is of the order of $10^6$ cm/s for all electrode materials investigated (Fig. 9). It is interesting that the regularities found for the closure time $t_c$ are the same for pulsed and dc vacuum discharges.

The regularities found for the closure time $t_c$ are accounted for by the expansion of the cathode plasma resulting from a microexplosion. Electron-optical records of the cathode glow (see Fig. 2) show plasma microblobs appearing a few nanoseconds after the application of voltage [4]. These microblobs, named cathode flares (CF), represent the plasma formed as a result of an explosion of the cathode material in surface microregions. Generally, a single or several CFs appear at the cathode, depending on the overvoltage across the gap. At a dc breakdown, only one CF appears. It has been shown [4] that the glow of the CF plasma is interrupted in character and for a copper cathode its periodicity is 3–5 ns. This may be an indication of disappearance of ectons and appearance of new ones at the cathode surface.

For copper, the velocity of motion of the cathode flare is about $1.6 \cdot 10^6$ cm/s. An investigation of the regularity of the EEE current rise has shown that this rise is limited by the space charge of the electron current emitted by CF. In the general form, this regularity is written as

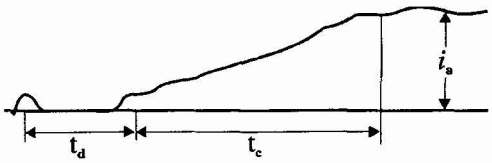


Fig. 8. Current waveform in vacuum discharge.

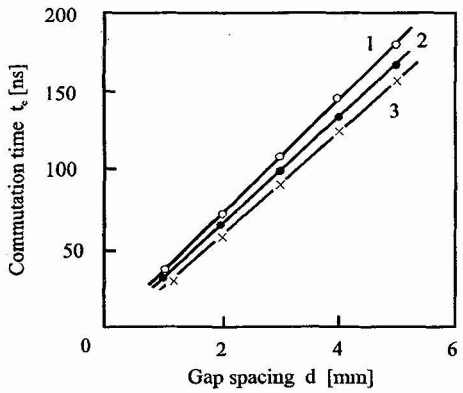


Fig. 9. Closure time *versus* vacuum gap spacing for electrodes made of aluminum (*1*), copper (*2*), and molybdenum (*3*).

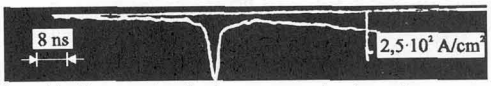


Fig. 10. Current density burst at anode along the discharge axis. $V = 30$ kV, $d = 4$ mm.

$$i = A_0 V^{3/2} F(vt/d), \tag{5.1}$$

where $A_0$ is a constant depending on the gap geometry, $V$ is the voltage between the cathode and the anode, v is the velocity of expansion of the cathode plasma, $d$ is the gap spacing, and $t$ is the time. For a single CF at a cathode of radius $r < vt$ with $d >> vt$ we have $F(vt/d) \propto vt/d$. For this case, the current rise rate at the initial stage of EEE is given by

$$\frac{di}{dt} \approx A_0 V_0^{3/2} \frac{v}{d} = A_0 V_0^{1/2} E_0 v, \tag{5.2}$$

where $E_0$ is the initial field in the gap. For $E_0 \approx 10^6$ V/cm, $v = 2 \cdot 10^6$ cm/s, $V_0 \approx 10^4$ V, and $A_0 \approx 3.7 \cdot 10^{-5}$ $AV^{-3/2}$, $di/dt$ will be on the order of $10^{10}$ A/s, as obtained in experiment [4]. The linear rise of the closure time $t_c$ on the gap spacing $d$ follows immediately from formula (5.1), as for a fixed current we have $vt_c/d$ = const and, hence, $t_c$ proportional to $d$.

After a time, in addition to the CF, an anode flare (AF) appears, which is due to the heating of the anode surface by the EEE current (see Fig. 2). This fact together with the existence of intense X-radiation at the anode during the time the CF moves toward the anode and the reflection of the beam by the magnetic field perpendicular to the electric field are strong evidence for the electronic character of the current emitted by the cathode after the appearance of an ecton at the cathode surface. An important information about ectons can be obtained by investigating the local current density at the anode. If we make a hole in the anode and measure the electron current, we may observe intense current bursts on the background of a monotonicly rising spark current [4]. This suggests that at local sites of the cathode new electron sources – ectons – appear. Figure 10 shows a current burst at the discharge axis for copper electrodes: a point cathode and a plane anode. The duration of this burst was ~10 ns. Current bursts of the same duration were observed for a voltage of 20–200 kV and gap spacings of 1–17 mm [4].

Examination of the microcraters formed on the cathode has revealed two types of microcraters. First, there are many craters at one and the same place. Second, there are craters located at a certain distance from one another. Both types of craters may be produced by a single discharge (Fig. 11). Craters of the first type appear due to the fact that liquid-metal jets interacting with plasma explode and produce new craters at the same place. Craters of the second type may be formed for two reasons: by several simultaneous microexplosions initiated by simultaneous Joule heating of several micropoints (as can be seen in Fig. 2) and by a plasma-initiated microexplosion occurring due to charging and breakdown of dielectric inclusions on the cathode surface or due to the effect of current density enhancement at microprotrusions flown over with plasma (see Sec. 4). A detailed study of the craters has been made by B. Juttner *et. al.* in a number of papers, which are generalized in a thesis [33].

We can estimate the existence time of EEE current, i.e., the existence time of an ecton, $t_e$, from the radius of a corresponding on the cathode surface crater ($r_c \approx 2 \cdot 10^{-4}$ cm). If the crater radius is related to heat conduction, it is found from the formula:

$$r_c \approx 2(at_e)^{1/2}. \tag{5.3}$$

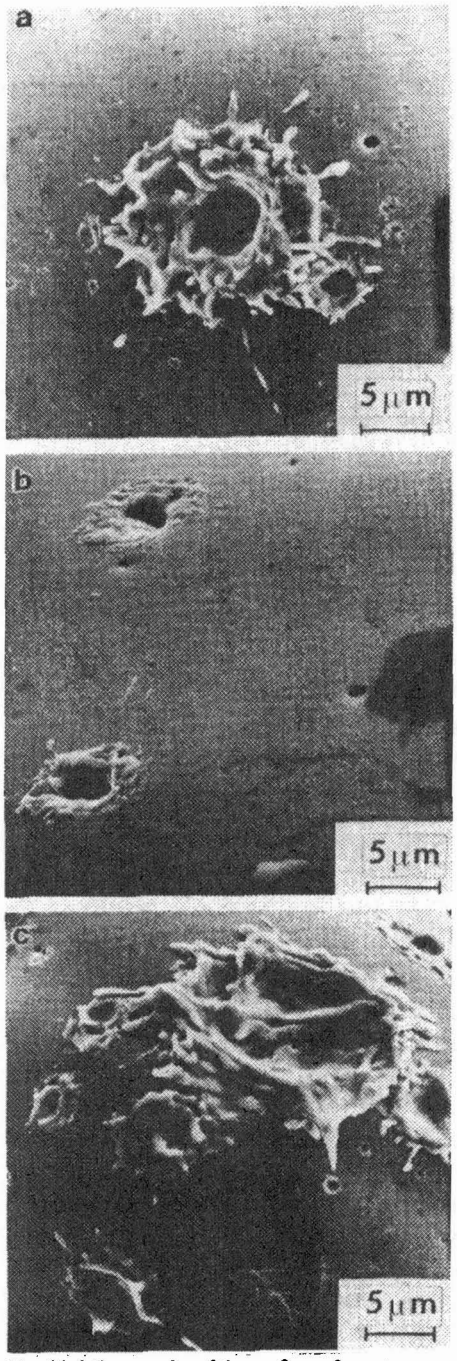


Fig. 11. Micrographs of the surface of a copper cathode after a single current pulse with $t_p = 20$ (*a*), 50 (*b*), and 100 ns (*c*); $d = 3$ mm, $V = 30$ kV.

We have $a \approx 1.6$ cm$^2$/s, and so $t_e \approx 6$ ns. About the same value of $t_c$ can also be inferred from the micrograph given in Fig. 11. Here, three craters have been formed at the same place within 20 ns. Therefore, the lifetime of each of them was ~ 6–7 ns. Important data about the spark stage of a discharge have been obtained in studying the ejection of drops from a cathode [4]. For a copper cathode, the reduced specific number of ejected drops has been obtained to be in average $\gamma_d \approx 2 \cdot 10^7$ C$^{-1}$. The maximum of the drop diameter distribution for the pulse duration ranging from 30 to 300 ns remained fixed and corresponded to the drop diameter ~ 0.1 μm. This is strong evidence in support of the cyclic nature of the processes occurring at the cathode in a vacuum discharge (see Fig. 10). If we assume that the appearance of drops is an element of an ecton cycle, this means that the duration of an ecton process is shorter than 10 ns (Fig. 12). Thus, we have found that $t_e \approx 5$–10 ns. From the foregoing, a model of a vacuum spark emerges as follows: After the appearance of a first ecton through spontaneous and secondary processes, new ectons appear whose number depends on the current and duration of the spark stage. If each ecton has a charge $q_e$ and one drop corresponds to one ecton, the charge of one ecton will be

$$q_e = 1/\gamma_d. \tag{5.4}$$

For $\gamma_d \approx 2 \cdot 10^7$ C$^{-1}$ we have $q_e \approx 5 \cdot 10^{-8}$ C. Since $q_e = i_e t_e$, then for $t_e = 5$–10 ns the ecton current will be ~ 5–10 A.

The number of ectons initiated during the spark stage, $N_0$, will be determined from the relation

$$N_0 \approx \int_0^{t_s} i\,dt / q_e = \gamma_d \int_0^{t_s} i\,dt, \tag{5.5}$$

where $t_s \approx t_c$ is the duration of the spark stage. Since the total charge transferred during the spark stage can be found approximately as $Q_s \approx t_s i_a$, where $i_a$ is the pulsed current amplitude, we have

$$N_0 \cong \gamma_d t_s i_a \approx \gamma_d i_a d / v_{ac}, \tag{5.6}$$

where $v_{ac}$ is the velocity with which the cathode plasma approaches the anode plasma. From Eq. (5.4) it follows that the number of electrons in an ecton is ~ $3 \cdot 10^{11}$.

For a current of 100 A, $d = 1$ cm, and $v_{ac} \cong 2 \cdot 10^6$ cm/s, the total number of ectons initiated during the spark stage will be, according to Eq. (5.6), $N_0 \cong 10^3$. Let us now estimate the reduced mass removed from the cathode in the spark stage of a vacuum discharge. According to Eq. (2.6), we have $\gamma_m = (2\rho/3)(a/\bar{h})^{1/2}$. The values of $a$ and $\bar{h}$ should be taken for molten metal. For copper we have $a = 0.47$ cm$^2$/s, $\bar{h} \cong 3 \cdot 10^9$ A$^2$s/cm$^4$, and $\rho = 8.9$ g/cm$^3$, and so $\gamma_m \cong 7.5 \cdot 10^{-5}$ C$^{-1}$. Measurements of $\gamma_m$ in a vacuum discharge with a cathode made of a cylindrical copper wire of diameter 50 μm and with a current rise rate of $(0.3–1.1) \cdot 10^9$ A/s have yielded in average $\gamma_m \cong 4 \cdot 10^{-5}$ g/C [4]. The difference between estimates and

measurements is perhaps related to the error involved in the determination of the charge from current oscillograms and to the use of the $a$ and $\bar{h}$ values corresponding to a solid-state metal for a liquid metal.

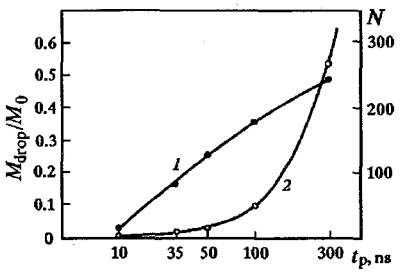


Fig. 12. Relative drop fraction mass (*1*) and number of drops (*2*) versus pulse duration for a copper cathode.

## 6. THE VACUUM ARC

The vacuum arc has some features making it different from other types of discharge. In its operation, there is a low potential difference which is localized in the cathode region and equals approximately the ionization potential of the cathode material. There is a threshold current at which an arc ceases to operate. The vacuum arc space between the cathode and the anode consists of three regions. One of them is at the cathode and looks like a bright luminous spot executing a fast random motion over the cathode surface. This region is called a cathode spot. Another region takes most of the space between the cathode and the anode and has the appearance of a bright diffuse glow. This region is referred to as a positive column and plays the role of a plasma conductor between the cathode and the anode. It is characterized by a uniform electric field distribution and a comparatively low potential gradient. At the anode, a region exists which is named an anode region. The peculiarity of the phenomenon of a vacuum arc is in fact associated with the cathode spot. The problem of studying the vacuum arc is reduced to the study of its cathode spot which, as mentioned above, is characterized by a high current density and a high energy concentrated in a unit volume. To initiate an arc in a vacuum between metal electrodes, it is necessary to fulfil some conditions. First of all, a certain minimum potential difference should be maintained, which, for short arcs, approaches the cathode fall voltage $V_c$. Moreover, an arc will operate if only the discharge current is over a threshold value, $i_{th}$, depending on the electrode material.

The now available techniques for the initiation of a vacuum arc are as follows [32]: initiation of breakdown in the vacuum gap with a fixed electrode separation, approaching the electrodes to one another, breaking the circuit, passing a current through a semiconductor immersed in liquid metal, inducing the glow-to-arc transition, producing a plasma flowing over the cathode surface, *etc.* We will not consider these techniques in detail but only note that all them are eventually reduced to the concentration of energy in a cathode microvolume and to the initiation of a primary ecton.

A cathode spot is a small bright luminous region over the cathode surface through which the current transfer between the cathode and the arc column occurs. In the spot region, the cathode surface is heated to a temperature being much over the boiling point of the cathode material. A recent review of the cathode spot studies has been made by [13]. Cathode spots come in two types [33]. A first-type cathode spot consists of individual bright spots located at a certain distance from one another. For these spots, the mass of the cathode material removed per unit charge is not large (for copper $\gamma_m = 5 \cdot 10^{-7}$ g/C). Spots like these appear due to the excitation of ectons on charging dielectric films and inclusions by the current of the plasma flowing over the cathode. This is so indeed since first-type spots do exist only at a cathode which has not been cleaned from contaminants. At a cathode thoroughly cleaned by heating, ion bombardment, or by other techniques, second-type spots appear which have large dimensions and consist of individual fragments. Furthermore, first-type spots, when operating for several hundreds of microseconds (with a current on the order of 100 A), change into spots of the second type. This can be accounted for by the fact that that within this time the cathode surface is cleaned from adsorbed gases and dielectric inclusions and films. For second-type spots, $\gamma_m$ is much greater (on the order of $10^{-5}$–$10^{-4}$ g/C).

Kesaev [32] has shown that a cathode spot contains individual cells which carry a current being not over than the doubled threshold current. When the current becomes higher than the doubled threshold current, it is observed that some cells cease to exist and new cells appear through division of the

remaining ones. The cathode spot ejects plasma, vapors, and drops of the cathode material. The appearance of a cell, its functioning and the following death make up an arc cycle.

We will proceed from the Kesaev's idea that a cathode spot consists of individual cells, each carrying a current equal to the doubled threshold arc currents: $i_m = 2i_{th}$. For copper we have $i_{th} \cong 1.6$ A. In our opinion, the functioning of a cathode spot cell is a typical ecton process. An ecton is formed as a result of the interaction of a molten-metal jet with plasma. Such jets are ejected from the cathode surface due to a high pressure in the microexplosion zone, which may reach $10^4$–$10^5$ atm [4]. For a current exceeding the threshold arc current, a liquid-metal jet forms a drop which, still before its break-off, provides an enhancement of the ion current density at the jet-drop joint. This results in concentration of energy at the joint and in a microexplosion initiated by Joule heating of the joint [1].

In our view, an arc cycle involves two processes (Fig. 13). The first one, whose duration is $t_e$, is the operation of an ecton, and the second one, whose duration is $t_i$, is associated with the ion current flowing in the cathode region. In Fig. 10, the time $t_e$ corresponds to the low-voltage stage and $t_i$ to the stage with an increased voltage. Let us use the notation $\alpha = t_i/t_e$. Within the time $t_e$, the ecton current flows and the formation of a new liquid-metal jet is completed. Within the time $t_i$, a new ecton is induced. Thus the process becomes self-sustaining.

For an ecton produced as described above, i.e., on detachment of a drop or with a drop being a constituent of an ecton cycle, the criterion for the arc cycle to be self-sustaining is written as

$$\gamma_d t_c i_m \geq 1, \tag{6.1}$$

where $\gamma_d$ is the number of drops produced per unit charge and $t_c = t_e + t_i$ is the time of the arc cycle, where $t_e$ is the electronic phase of the cycle and $t_i$ is the ionic phase of the cycle. Assume that a liquid-metal jet has the shape of a cone [10, 34]. Then the ecton lifetime and the mass of the metal removed from the cathode will be determined from formulas (2.3) and (2.4) with $i = 2i_{th}$. For an arc, the reduced mass removed from the cathode is given by

$$\gamma_m = \frac{2}{3}\rho(1-\alpha)\left(\frac{a}{\bar{h}}\right)^{1/2}. \tag{6.2}$$

For copper we have $\alpha \cong 0.2$, $a = 0.42$ cm$^2$/s, $\bar{h} \simeq 3\cdot10^9$ A$^2$·s/cm$^4$ [10, 34] and, hence, $\gamma_m \approx 0.6\cdot10^{-4}$ g/C. Daalder [35] in his experiments obtained $\gamma_m \approx 0.4\cdot10^{-4}$ g/C. Studies of the vacuum discharge have shown that the explosion of micropoints on the cathode is accompanied by ejection of cathode plasma which propagates toward the anode with a velocity v > $10^6$ cm/s [4]. This results in the appearance of a positive ion current flowing toward the anode, $i_i$, (anode erosion) whose fraction in the total arc current is

$$i_i/i = \gamma_m q Z e / m_a, \tag{6.3}$$

where $i$ is the arc current, $q$ is an average ion charge, $Z$ is the degree of ionization of the plasma, $m_a$ is the atomic mass, and $e$ is the charge of an electron. According to the data of Kimblin [36], $Z = 0.55$ and the average charge $q = 1.5$ [37] or 1.85 [38]. We take an averaged value: $q = 1.7$. Substitution of $\gamma_m$ determined from Eq. (6.2) into Eq. (6.3) yields $i_i \approx 0.08i$, which agrees with the experimental data of Kimblin [36]. For further estimates it is necessary to know the cone angle $\theta$. For known $\alpha$ and $t_c$ we can find $t_e$ and determine $\theta$ from Eq. (2.3). For our case we have $\theta \approx 0.53$. The cone angle can also be found knowing the reduced number of drops $\gamma_d$ ejected by the vacuum arc cathode spot. For instance, for silver we have $\gamma_d \approx 1.4\cdot10^7$ C$^{-1}$ [39]. According to Eq. (6.2), for $i_{th} = 1.6$ A we obtain the time of the cycle $t_c \approx$ 22 ns, which is close to the value measured from potential oscillations. For the general case, substituting


Fig. 13. Arc cathode potential oscillations for a copper cathode with a current of 4 A.

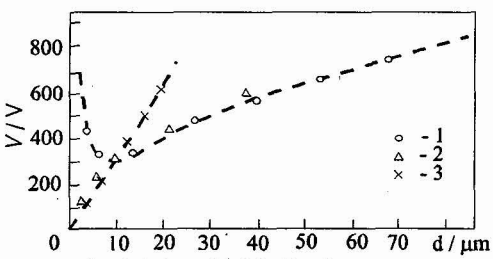


Fig. 14. The right branch of the Paschen curve $V = f(pd)$ for air (*1*) and hydrogen (*2*) [45].

(6.1) into (2.3), we obtain

$$\theta^4 \approx \frac{1}{\pi^2(1-\alpha)} \frac{i_m^3 \gamma_d}{a^2 \bar{h}}. \tag{6.4}$$

From Eq. (6.4) it follows that $\theta = 0.54$. Now we dwell on the estimation of the arc current density. It is different for different points in time. The current density at the instant an ecton is initiated will be found from the relation $j^2 t_d = \bar{h}$. Since we have $\bar{h} \approx 10^9$ A$^2$s/cm$^{-4}$, the time delay to explosion is $t_d \approx 10^{-9}$ s. For the instant the ecton ceases to operate, the current density will be determined from the formula

$$j_e = \pi a \bar{h} \theta^2 / i_m. \tag{6.5}$$

For copper it will be $2.2 \cdot 10^8$ A/cm$^2$. However, the current density is commonly estimated from the measured radius of the crater, $r_c$, on the cathode surface and from the arc current. Estimation of the crater radius by the formula $r_c = 2(at_c)^{1/2}$ yields $r_c \approx 2 \cdot 10^{-4}$ cm, which is close to the data of [40] for arc currents $i < 10$ A. For this case, the apparent current density defined as $j_c = i_m/(\pi r_c^2)$ will be $2.7 \cdot 10^7$ A/cm$^2$. This is close to the measured value for copper [40]. Based on the ecton mechanism of a vacuum arc, the Tanberg effect [41] can be explained. This effect is that during the operation of an arc, a force acts on the cathode that seeks to increase the distance between the cathode and the anode. The Tanberg effect is characterized by a parameter, $f$, which is the force per unit current:

$$f = m_e v/(2t_c i_m), \tag{6.6}$$

Here, v is the velocity of the cathode plasma. According to Tanberg [41], for copper this velocity is ~$10^6$ cm/s. The number two in Eq. (6.6) accounts for the anisotropy of the plasma expansion. In view of the relation $m_e/(t_c i_m) = \gamma_m$, we have

$$f = \frac{\rho v}{3} \left( \frac{a}{\bar{h}} \right)^{1/2}. \tag{6.7}$$

For copper we obtain $f \approx 30$ dyn/A. The experimental data of Tanberg yield 20 dyn/A for the reduced force. The above results show that the ecton mechanism offers a satisfactory explanation to the operation of the cathode spot of a vacuum arc. The threshold current, the cathode fall potential, the plasma jet velocity, and other parameters of the arc phenomena are explained in terms of the ecton mechanism in our works [1, 4, 34]. Interesting evidence for the existence of cyclic processes in an arc is also provided in [42].

## 7. ECTONS IN A GAS DISCHARGE

### 7.1 Departure from the Paschen law

We think ectons play an important part in many types of electrical discharge in gases. The appearance of ectons has the result that the classical discharge mechanisms are violated. The reasons for the appearance of ectons at the cathode are the same for gas and vacuum discharges. They are the explosion of cathode microprotrusions caused by the high FE current resulting from a high electric field at the cathode and the breakdown of dielectric films and inclusions present on the cathode surface due to their charging by ions from the discharge plasma. On the one hand, the gas present in the discharge gap facilitates the initiation of ectons owing to the existence of the gas discharge plasma and the dielectric films formed as a result of the interaction of the gas and the metal. On the other hand, a microexplosion at the cathode surface is not necessarily accompanied by a fast rise of the current because present an obstacle to the current rise the atoms and molecules met by the ecton electrons in their motion. A manifestation of the ecton processes is the violation of similarity laws, in particular, in the Paschen law. The latter relates the statistical breakdown voltage, $V$, to the gas pressure, $p$, and the gap spacing, $d$, as $V = f(pd)$.

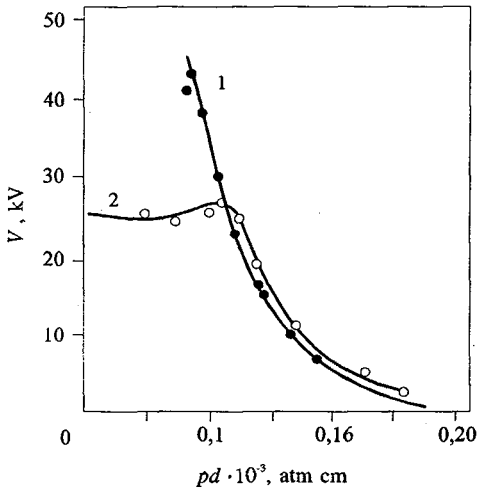


Fig. 15. The left branch of the Paschen curve: (*1*) classical dependence and (*2*) dependence in the presence of an ecton [43].

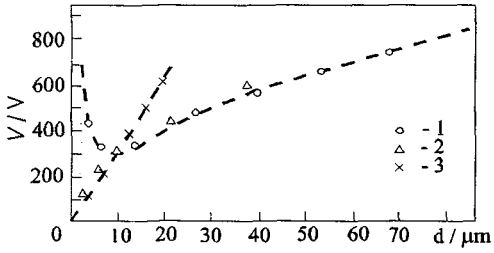


Fig. 16. Neighborhood of the minimum of the Paschen curve: (*1*) points on the Paschen curve; (*2*) points of deviation from the Paschen curve, and (*3*) points corresponding to the average electric field $3 \cdot 10^5$ V/cm [43].

A departure from the Paschen law is generally observed for three portions of the Paschen curve: the right branch corresponding to high pressures, the left brunch corresponding to low pressures, and the region of the minimum. For all these portions, the average electric field in the gap is high enough (on the order of $10^6$ V/cm and more) for FE to occur from individual cathode microprotrusions. The emitted electrons ionize the gas and the resulting ions move toward the cathode. With that, FE is enhanced by the ion space charge, which further increases the FE current density. Eventually, all this leads to the formation of ectons. As can be seen from Figs. 14, 15, and 16, any departure from the Paschen curve results in a decrease in breakdown voltage compared to the breakdown voltage determined by the Paschen law.

### 7.2 Constriction of a volume discharge

Another manifestation of the ecton processes in a gas discharge is the constriction of the discharge, i.e., its transition from spatial to channel operation [43]. Examples of space discharges are the low-pressure glow discharge, the self-sustained pulsed space discharge operating at both low and high pressures (1 atm and more), and, finally, the non-self-sustained discharge with intense external ionization, e.g., by an electron beam [44].

For space discharges, the discharge constriction begins directly at the cathode because of the initiation of an ecton by FE current or by breakdown of the dielectric film present on the cathode surface. In view of the fact that discharges of all mentioned types constrict in the same manner, we consider this effect for a glow discharge as an example.

Characteristic features of a glow discharge are the spatial character of the current flow and the presence of a cathode fall potential layer owing to which electrons from the near-cathode regions come uniformly into the discharge column. The potential fall across the near-cathode regions is typically equal to several hundreds of volts and the size of the near-cathode region is established such that conditions for the discharge to be self-sustaining are provided through ionization processes in the gas and through secondary processes at the cathode.

The secondary electrons appear at the cathode on its bombardment by positive ions, due to photoeffect, and on bombardment of the cathode by fast neutral atoms resulting from charge exchange and other processes. These processes provide, as a rule, a uniform current density of secondary electrons at the cathode and, correspondingly, a homogeneous structure of the cathode layer. For a normal glow discharge, the current density remains constant, while the total current increases due to the increase in the area taken by the discharge at the cathode. Once the discharge has taken the entire surface, further increase in the total current in the circuit results in an increase in its density and in discharge operating voltage. The glow discharge in this case is said to operate in an abnormal mode. As a certain current density is achieved in an abnormal discharge, this results in a jumpwise glow-to-arc transition.

The glow-to-arc transition is accompanied by redistribution of the current in the discharge column (column constriction) and of the current at the cathode (current localization in the cathode spot region). There are two viewpoints on the mechanism of the glow-to-arc transition.

One viewpoint implies that the discharge constriction is due to the instabilities appearing in the discharge column. For instance, for a glow discharge operating in a long tube, the column may constrict owing to the fact that more energy is released at the axis than in the peripheral regions. This results in heating of the gas and in a decrease in the density of neutrals. The decrease in neutral density in turn leads to more intense power dissipation at the discharge axis [46, 47].

However, another approach also exists which is based on experimental data on the instabilities developing in the near-electrode regions (more often in the cathode region) and causing the discharge to constrict [43]. It is believed that these instabilities are responsible for the instability of the discharge column. This viewpoint is less represented in the literature. Even in early experiments, both the radial constriction of the column of a glow discharge, with the cathode layer parameters being unchanged, was observed as the current reached its critical value [48] and arcing induced by the instabilities having developed in the cathode region was detected [49]. With that, the second mechanism was realized over a wide range of experimental conditions, at high and at low gas pressures.

In accordance with the concept being developed in this review, one type of instability may occur in the cathode region if the electric field at the cathode is high enough for FE to be initiated at separate regions of the surface. The FE current is then enhanced by the space charge of positive ions which leads to further increase in current density, explosion of micropoints, and formation of ectons.

### 7.3 The corona discharge

A corona discharge is generally realized with a point–plane electrode geometry. A high electric field (over $10^5$ V/cm) takes place at the point tip at which the corona starts developing. Depending on the polarity of the electrode with a small radius of curvature, the corona discharge may be either positive or negative. The electric field at the point tip is defined as $E \approx V/r$, where $r$ is the radius of curvature of the point tip and $V$ is the potential at the point. At a high field near the point, the gas is intensely ionized since the coefficient of impact ionization strongly depends on electric field. From the data reported elsewhere [45] it can be concluded that some effects observed in a negative corona may be treated as ectons. First, at the cathode of a negative corona, bright cathode spots are observed. Second, Meek and Craggs [45] paid attention to holes appeared on the negative point with coronas operating in nitrogen and hydrogen. In the experiment described in [45], positive ions that reached the cathode had energies not over 1 eV; therefore, the appearance of "craterlike holes" seemed very strange. This phenomenon was observed for tungsten, platinum, copper, and lead electrodes. Now this effect can be interpreted through the appearance of ectons.

The initiation of ectons at the stage of the formation of a corona discharge in air was observed by Gamdling [48]. His experiments were performed in the main with an electrode gap of spacing 0.6 cm to which strictly single rectangular pulses of controllable duration were applied. The initial voltage was 25 kV and the voltage risetime was $10^{-9}$ s. The radius of the point tip was 1 mm and more. The opposite electrode was a hemisphere of radius 0.3 cm. After breakdown, the point surface was examined in a scanning electron microscope. Moreover, the state of the test points was judged by viewing them through a shadow electron microscope. With a pulse of duration 3 ns, a crater appeared regardless of the polarity of the voltage applied to the point. However, for points of larger radius, a spot was initiated if only the point was a cathode. With that, erosion marks having the form of microcraters were observed on the cathode. The initiation of ectons at a cathode is accounted for by the development of a cathode instability. This is confirmed by the unlike character of the surface damage for the cathode and the anode. The cathode surface damage looks like grouped molten balls 1–2 μm in diameter which more often are

closely packed within a region of size 20–30 μm. This means that, like in a vacuum discharge, ectons are initiated at microirregularities of the cathode surface, appearing at the edges of the craters produced by preceding breakdowns. For a point whose polarity is negative, a cathode spot is initiated within a time $t < 3$ ns. The current density at the anode increases with pressure and for a pulse duration of 20 ns and a pressure of 76, 152, and 228 mm/Hg it is equal to $1.3 \cdot 10^4$, $2.6 \cdot 10^4$, and $5 \cdot 10^4$ A/cm$^2$, respectively. Putting for the electron drift velocity v = $10^7$ cm/s, we obtain that the electron density in the widest part of the diffuse channel near the anode is on the order of $10^{16}$ cm$^{-3}$.

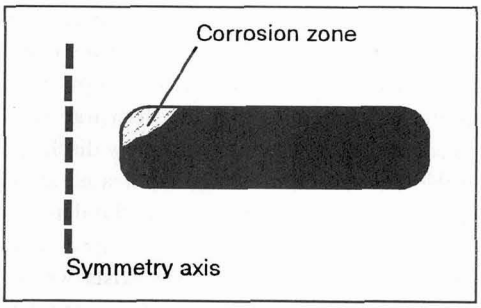


Fig. 17. Schematic view of a molybdenum cathode after $5 \cdot 10^6$ breakdowns for a discharge of duration 90 ns and current 20 kA [52].

### 7.4 The pseudospark discharge

In the recent decade, the pseudospark, a variety of the high-current space discharge, has been studied extensively [50]. This is a discharge with a hollow cathode and a hollow anode. It is initiated in high-current switches, which outperform thyratrons, and in electron sources. Of particular interest for this type of discharge is the emission mechanism that provides an average current density of $10^4$ A/cm$^2$. The principal characteristics of pseudosparks are as follows: the gas pressure in the spark gap is typically $p \approx$ 0.1 mm Hg, the gap spacing $d \approx 0.1$–1 cm, and the free path of an electron in the gap between the electrode $\lambda_e > d$. Once a discharge has been initiated in the hollow cathode, the plasma produced enters the zone of the hole, and an electron beam is formed whose current reaches 10–100 A. At this stage, the gas present on the cathode surface is desorbed and then ionized, and the plasma density in the region of the hole reaches of the order of $10^{16}$ cm$^{-3}$. The diameter of the luminous channel is approximately equal to the diameter of the hole [50]. A high-current discharge with a current density of $10^4$ A/cm$^2$ is formed when the plasma glow expanding in radius with a velocity of $10^8$ cm/s [50] fills the electrode gap to a size equal to five or six point diameters. The voltage across the discharge falls to several hundreds of volts. This voltage is localized across a layer of thickness $10^{-4}$ cm and induces the field at the cathode $E = (1–5) \cdot 10^6$ V/cm [50]. Thermal electron emission is generally assumed as the most probable emission mechanism. To produce the current density $j = 10^4$ A/cm$^2$ at the electric field $E = (2–5) \cdot 10^6$ V/cm, the cathode temperature $T$ should be over 3500 K. For this temperature to be achieved for a molybdenum cathode within a time $t < 50$ ns (the formative time of a high-current discharge), the power density at the cathode should be $(3–4) \cdot 10^7$ W/cm$^2$. However, the most optimistic predictions yield the energy flux intensity not over $10^6$ W/cm$^2$, which is evidently insufficient to heat the cathode to the melting point. The cathode microrelief after the operation of a pseudospark looks like the relief formed as a result of the action of an arc discharge [50]. The cathode material mass removed per unit charge for molybdenum is $(5–8) \cdot 10^{-5}$ g/C, which is typical of an ecton process. The metal erosion is most intense at those places where the electric field is high, i.e., at the cathode edge (Fig. 17). In view of the character of the cathode damage, there are strong grounds for believing that the high average current density in pseudosparks is provided by ectons.

The study of the physical processes involved in the initiation and development of vacuum breakdown and the mechanisms for the emission in the cathode spot of a vacuum arc and in a space gas discharge has made it possible to establish some regularities proving that the mechanism for the emission in a pseudospark is conditioned by ectons [51]. We will proceed from the fact that the average current density on the order of $10^4$ A/cm$^2$ in a pseudospark can be provided by $10^3$ ectons, each carrying a current

of 10 A. The current density in an ecton may reach $10^8$ A/cm$^2$. The appearance of ectons within the time td takes place provided that $j^2 t_d$ = const. For an initial current density of $10^9$ A/cm$^2$, the time $t_d$ is in the nanosecond range. It has been shown [4] that for a molybdenum cathode conditioned in high vacuum with the average electric field at the cathode $E > 2 \cdot 10^6$ V/cm, we have $t_d \sim 1$ ns. The field produced by a space discharge at the initial stage of the formation of a pseudospark is of the same order of magnitude, and, hence, there exist prerequisites for the formation of an ecton within a time $t < 10$ ns.

## 8. CONCLUSION

The present paper shows that in a number of electric gas and vacuum discharges, a fundamental role attaches to ectons. These are short-term electron avalanches emitted by the cathode for $10^{-9}$–$10^{-8}$ s. Ectons arise from the overheating and explosion of microvolumes near the surface of the cathode, owing to Joule heating or other effects (laser beam, the impact of a microparticle, the action of the plasma, etc.). After a primary ecton has been initiated, secondary ectons may appear if the current exceeds the threshold current. Secondary ectons emerge from the explosion of jets of liquid metal as they interact with the plasma produced by the preceding ecton. We have provided conclusive evidence for the role of ectons in a vacuum discharge (breakdown, spark, arc). As regards the gas discharge, especially at a high gas pressure, our statement here is a hypothesis. An ecton theory is currently difficult to create because as an ecton is produced the cathode material in a volume $10^{-12}$ cm$^3$ passes from the solid to the liquid, vapor and plasma entity in no more than $10^{-8}$ s. The semiclassical estimates that we have made by invoking the quantity "specific action" give a fairly good fit to experimental data. We hope that our paper will give an impetus to studying a phenomenon such as the ecton and its role in electric discharges.

### References


[1] Mesyats G.A., *Pisma Zh. Eksper. Teor. Fiz.* **57** (1993) 88-92.

[2] Mesyats G.A. and Proskurovsky D.I., *Pisma Zh. Eksper. Teor. Fiz.* **13** (1971) 7-10.

[3] Mesyats G.A., "The role of fast processes in vacuum breakdown", X Int. Conf. on Phenomena in Ionized Gases, Inv. Pap., (Oxford, 1971) p. 333.

[4] Mesyats G.A. and Proskurovsky D.I., Pulsed Electrical Discharge in Vacuum (Springer-Verlag, Berlin–Heidelberg, 1989).

[5] Burtsev V.A., Kalinin N.V., and Luchinsky A.V., Electrical Explosion of Conductors, (Energoatomizdat, Moscow, 1990).

[6] Fortov V.E. and Yakubov I.T., Nonideal Plasmas (Energoatomizdat, Moscow, 1994).

[7] Sedoi V.S., Chemezova L.I., Chernov A.A., Megagauss Fields and Pulsed Power Systems (Nova Science, New York, 1990).

[8] Vitkovitsky I.M., High Power Switching (Van Nostrand Reinhold Comp., New York, 1987).

[9] Juttner B., Puchkarev V.F., Rohrbeck W. "Behavior of Micropoints During High Voltage Vacuum Discharges", VII Int. Symp. on Discharges and Electrical Insul. in Vacuum (ISDEIV) (Novosibirsk, 1976) p. 189.

[10] Mesyats G.A., *IEEE Trans. on Plasma Science* **23** (1995) 879.

[11] Zel'dovich Ya.B. and Raizer Yu.P., Physics of Shock Waves and High-Temperature Hydrodynamic Phenomena (Nauka, Moscow, 1966).

[12] Vogel N. and Skvortsov V., "Plasma Parameters within the Cathode Spot of Laser-Induced Vacuum Arcs: Experimental and Theoretical Investigations", XVII ISDEIV (Berkeley, 1996) pp.89-98.

[13] Handbook of Vacuum Arc Science and Technology, Ed. by R.L. Boxman, P.J. Martin, and D.M. Sanders (Noyes Publications, New York, 1995).

[14] Little R.P. and Whitney W.T., *J. Appl. Phys.* **34** (1963) 2430-2432.
[15] Nadgorny E.M., Osip'yan Yu.A., Perkas M.D., *Usp. Fiz. Nauk* **67** (1959) 625-662.
[16] McDaniel E.W., Collision Phenomena in Ionized Gases (John Wiley & Song Inc., 1964).
[17] Cox B.M., *J. Phys. D* **8** (1975) 2065-2073.
[18] Gopra K.L., Electrical Phenomena in Thin Films (Mir, Moscow, 1972).
[19] Vorobjov G.A. and Mukhachev V.A., Breakdown of Thin Dielectric Films (Sov. Radio, Moscow, 1977).
[20] Boyle N.S., Kisliuk K.P., and Germer L.H., *J. Appl. Phys.* **26** (1955) 730.
[21] Dyke W.P., Trolan J.K., Martin E.E., *Phys. Rev.* **91** (1953) 1043.
[22] Alpert D., Lee D.A., Lyman E.A., *J. Vacuum Sci. and Technol.* **1** (1964) 35.
[23] Elinson M.I. and Vasiliev V.G., Field Emission (GIFML, Moscow, 1958).
[24] Dyke W.P., Trolan J.K., Martin E.E., *Phys. Rev.* **5** (1951) 1054.
[25] Fursei G.N., Doctoral (Phys. & Math.) Thesis (Inst. of Semiconductor Physics, Novosibirsk, 1973).
[26] Tonks L., *Phys. Rev.* **48** (1935) 562.
[27] Pranevicius L., Serzentas S., and Bartasius J., "Liquid cathodes to study high voltage breakdown", VII ISDEIV (Novosibirsk, 1976) p. 234.
[28] High Voltage Vacuum Insulation, ed. by R. Latham (Academic Press, New York – Tokyo, 1995).
[29] Juttner B., *Plasma Sci,* **PS-15 5** (1987) 474.
[30] Shwizke F., Taylor R. *J. Nucl. Mat.* **93-94** (1980) 780.
[31] Seikov I.N., High-Voltage Processes in Vacuum (Energoatomizdat, Moscow, 1986).
[32] Kesaev I.G., Cathode Processes in Electric Arcs (Nauka, Moscow, 1968).
[33] Juttner B., Katodenprozesse Electrischer Enladung in Vakuum (Berlin, ZIE, 1981).
[34] Mesyats G.A., *Pisma Zh. Tekh. Fiz.* **60** (1994) 514-517.
[35] Daalder J.E., *J. Phys. D* **8** (1975) 1647-1659.
[36] Kimblin C.W., *J. Appl. Phys.* **44** (1973) 3074-3081.
[37] Davis W.D. and Miller H.C., *J. Appl. Phys.* **40** (1969) 2212
[38] Plyutto A.A., Ryzhkov V.N., and Kapin A.T., *Zh. Eksper. Teor. Fiz.* **47** (1964) 494-507.
[39] Utsumi T. and English J.H., *J. Appl. Phys.* **46** (1975) 126-131.
[40] Daalder J.E., *IEEE Trans. Pow. Suppl. Syst.* **93** (1974) 1747-1757.
[41] Tanberg R., *Phys. Rev.* **35** (1930) 1080.
[42] Juttner B., *J. Phys. D* **30** (1997) 221.
[43] Korolev Y.D. and Mesyats G.A., Physics of Pulsed Breakdown in Gas (Nauka, Moscow, 1991).
[44] Bychkov Yu.I., Korolev Yu.D. and Mesyats G.A., *Usp. Fiz. Nauk* **126** (1978) 451.
[45] Meek J.M. and Craggs J.D., Electrical Breakdown of Gases (Clarendon Press, Oxford, 1953)
[46] Ecker G., Kroll W., and Zoller O., *Phys. Fluids* **7** (1964) 2001.
[47] Jacob J. and Mani S.A., *Appl. Phys. Lett.* **26** (1975) 53.
[48] Gamdling W.A. and Edels H., *Nature* **177** (1956) 1090.
[49] Boyle W.S. and Haworth F.E., *Phys. Rev.* **101** (1956) 935.
[50] Gundersen M.A. and Schaefer G., Physics and Application of Pseudosparks, NATO ASI, Ser. B, (Plenum, New York, 1989)
[51] Mesyats G.A. and Puchkarev V.F., "On mechanism of emission in pseudosparks", XV ISDEIV (Darmstadt, 1992) p. 488.